CDF/PHYS/BOTTOM/PUBLIC/3270
Proceedings: HF95 Pisa.
July 21, 1995

Quarkonia production at Fermilab

CDF Collaboration

A.Sansoni

Istituto Nazionale di Fisica Nucleare, Frascati (RM) Italy.

Abstract

Recent data on J/ψ ,$\psi(2S)$,χ_c and Υ production has unraveled unexpected features of $Q\bar{Q}$ bound states production in high energy hadronic collisions.

In the 1992-1995 runs CDF has collected large samples of J/ψ ,$\psi(2S)$ and Υ identified through their muonic decay. In the charmonium system all production sources have been separately measured and compared with the theoretical predictions. A large excess of direct production has been observed for both $\psi(2S)$ and J/ψ . The relative production rate for the χ_c^1 and χ_c^2 has also been measured.

Results on J/ψ ,$\psi(2S)$ and χ_c production from the fixed target experiments E789,E705 and E672/706 are also presented. Important features of the production of charmonium states are shared by fixed target and collider data.

1 Introduction

The production of $Q\bar{Q}$ bound states in high energy collisions has recently been the subject of renewed theoretical interest. This is due to the fact that the experiments have measured the production cross sections for a wide variety of $Q\bar{Q}$ states and, for the $c\bar{c}$ system, they have been able to disentangle all the sources of production thus allowing a strict comparison with the theoretical prediction.

The large mass of the c quark ($m_c \sim 1.5 GeV/c^2$) implies that bound $c\bar{c}$ states are the first systems where perturbative QCD is expected to be applicable. At leading order,$O(\alpha_s^3)$, the production of a quarkonium state is described by the production of a free, color singlet, $Q\bar{Q}$ pair with the same quantum numbers of the quarkonium state [1]. The formation of the bound state is a non perturbative process that can be factored into a parameter either calculable within potential models or extracted from experimental data. Recently this picture has been improved with the inclusion of the process where a high p_T parton fragments into a color singlet $Q\bar{Q}$ pair [2]. This is an $O(\alpha_s^4)$ process but the extra p_T^2/m_Q^2 factor makes this the dominant one at high p_T .

In the $c\bar{c}$ system, high energy collider and fixed target experiments have measured the production of J/ψ ,$\psi(2S)$ and χ_c states. The predictions based on this model [1, 3] were that the χ_c have by far the largest cross section. Direct production of both J/ψ and $\psi(2S)$ was expected to be small because the extra gluon directly coupled to the $c\bar{c}$ line suppress this diagram. The χ_c^0 has a negligible branching ratio into J/ψ therefore prompt J/ψ were expected to originate almost completely from the radiative decays of the χ_c^1 and χ_c^2 . Feed-down is not relevant for the $\psi(2S)$ since the $\psi(2S)$ is heavier than the χ_c 's.

In collider experiments $c\bar{c}$ states can also arise from the decay of b flavored hadrons (this mechanism is negligible for fixed target experiments). This, non-prompt component, was expected to be the dominant source of $\psi(2S)$ and to contribute significantly to J/ψ production.

Prior to the successful operation of the CDF Silicon Vertex Detector, collider data were not inconsistent with this picture [4]. Fixed target and ISR collider experiments (no b production), on the other hand, reported already many years ago that χ_c 's were not the primary source of J/ψ [5] in disagreement with the expectations of the color singlet QCD model.

2 Quarkonia production at CDF

The data presented here are from $p\bar{p}$ collisions at $\sqrt{s} = 1.8\ TeV$ collected with the CDF detector in the 1992-1995 runs. The detector has been described in detail elsewhere [6]. The features most important for these analysis are: 1) the large tracking system contained in the 1.4 T axial magnetic field providing the high resolution momentum measurement of charged particles, 2) the 4-layer Silicon Vertex Detector (SVX) [7] providing the identification of secondary vertices associated with b decays, 3) the Pb-scintillator central electromagnetic calorimeter with a strip chamber embedded at a depth of 5.9 radiation lengths used for the photon reconstruction and 4) the muon chamber system, surrounding the central calorimeter, for the muon identification in the range $|\eta| < 1.0$.

The J/ψ ,$\psi(2S)$ and Υ 's are reconstructed using their muonic decay. The cutoff associated with the steel of the central calorimeter is $p_T(\mu) > 1.5\ GeV/c$. The level 1 trigger efficiency rises from 50% at $p_T(\mu) = 1.6\ GeV/c$ to 90% at $p_T(\mu) = 3.1\ GeV/c$. This implies that only relatively high p_T J/ψ can be reconstructed while, due to its larger mass, Υ 's can be reconstructed down to almost zero p_T . The event selection required:

- Two opposite sign good quality central muons
- $p_T > 2.0\ GeV/c$ for the soft μ

- $p_T > 2.8\ GeV/c$ for the hard μ
- $p_T^{\mu\mu} > 4.0\ GeV/c$ and $\mid \eta \mid < 0.6$ for J/ψ and $\psi(2S)$
- $p_T^{\mu\mu} > 0.5\ GeV/c$ and $\mid y \mid < 0.4$ for Υ 's

After this selection we observe a very clean signal of about 180,000 J/ψ in $75pb^{-1}$ of data. Cross sections are obtained correcting for acceptance and reconstruction efficiencies. The geometric and kinematical acceptances are determined from Monte Carlo simulations. The trigger and reconstruction efficiencies are measured from the data.

2.1 $\psi(2S)$

We first review the $\psi(2S)$. In $18pb^{-1}$ we observe 896 ± 94 $\psi(2S) \rightarrow \mu^+\mu^-$, with a signal to background ratio of 0.57. The measured production cross section is $\sigma(\mid \eta \mid < 0.6,\ p_t > 4.0\ GeV/c) = (94 \pm 8 \pm 9.3 \pm 21(Br))$ nb where (Br) is the systematic uncertainty associated with the decay branching ratio.

The first problem consists in separating between prompt production and feed-down from b decays. In the previous analysis [4] it was impossible to do this experimentally, therefore, following the theoretical prejudice, it was assumed that all $\psi(2S)$ came from b decays and b a cross section was derived. Now, with the CDF Silicon Vertex Detector, the prompt and long lived component can be precisely measured.

For each $\psi(2S)$ candidate reconstructed in the SVX the two dimensional decay length L_{xy} is calculated. L_{xy} is the projection of the vector $\vec{X}$, pointing from the primary to the secondary vertex, onto the transverse momentum vector of the $\psi(2S)$. The position of the secondary vertex is obtained by constraining the two muons to come from a common decay point. To convert L_{xy} into a proper lifetime we use $(\beta\gamma)$ of the $\psi(2S)$ and a correction factor F_{corr}, determined from Monte Carlo, to take into account the difference with $(\beta\gamma)$ of the b hadron.

$$L_{xy} = \vec{X} \cdot \vec{P_t}/P_t$$

$$c\tau_{pseudo} = \frac{L_{xy}}{(P_t/M) \cdot F_{corr}}$$

Figure 1 shows the $c\tau_{pseudo}$ distribution for the $\psi(2S)$. To determine the fraction from b's we fit this distribution with the sum of three contributions: 1) the prompt component parametrized with a gaussian, 2) the long lived component parametrized with an exponential smeared with the detector resolution (hatched in Fig.1) and 3) the background component obtained from the sidebands of the $\psi(2S)$ (dark shading in Fig.1). The result is that $22.8 \pm 3.5\%$ of the $\psi(2S)$ come from b decays, by far the majority is unambiguously prompt.

The statistics are sufficient to do this fit in several p_T bins, the fraction of $\psi(2S)$ from b's slowly increase with p_T . From this measurement we derive the differential cross section for $\psi(2S)$ from b's and for prompt $\psi(2S)$. This is shown in Figure 2 together with the theory curves. The b component is in reasonable agreement with the NLO QCD theory prediction while the prompt component is about a factor of 50 over the theoretical curve [3].

This large discrepancy, nicknamed the "CDF $\psi(2S)$ anomaly", has prompted the proposal that charmonium states above the $D\bar{D}$ threshold, whose decay in open charm is forbidden, or new exotic states, decay in $\psi(2S)X$ accounting for the excess [8]. Another proposal is that an additional mechanism, such as the production of a color octet $c\bar{c}$ state evolving non-perturbatively into a $\psi(2S)$ bound state, must be present in charmonium production [9]. To better understand the origin of this discrepancy it is natural, from the experimental point of view, to see if this excess is a feature of the $\psi(2S)$ only or it is also found in J/ψ production.

2.2 J/ψ

For the J/ψ the integrated production cross section is $\sigma(\mid \eta \mid < 0.6,\ p_t > 4.0\ GeV/c) = (487 \pm 3^{+51}_{-47} \pm 20(Br))$ nb. The prompt and b component are measured with the SVX fitting the $c\tau_{pseudo}$ distribution in the same way described for the $\psi(2S)$. The fraction of J/ψ from b's is $19.6 \pm 1.5\%$, similar to the $\psi(2S)$, and the cross section of J/ψ from b's is also in decent agreement with theory. Combining the cross section and fraction measurements for J/ψ and $\psi(2S)$ we derive the ratio of cross sections of $\sigma(\psi')/\sigma(\psi) = 0.19 \pm 0.05$ for promptly produced $\psi(2S)$ and J/ψ with $p_t > 4.0\ GeV/c$ and $\mid \eta \mid < 0.6$.

The prompt J/ψ cross section is again underestimated by the theoretical prediction, although only by a factor of ~ 6. But in this case the the prompt component includes both direct J/ψ production and feed-down from χ_c . It is therefore important to compare data and theory for the prompt and χ_c components separately. This can be done reconstructing the $\chi_c \rightarrow J/\psi\ \gamma$ decay and measuring the fraction of J/ψ that originates from this source.

The χ_c analysis is based on $32,642 \pm 181$ J/ψ candidates reconstructed in about $20 pb^{-1}$ of data. To reconstruct the $\chi_c \rightarrow J/\psi\ \gamma$ we combine the J/ψ with photon candidates found in the event. A photon candidate is defined by a central electromagnetic calorimeter tower with energy $E^{\gamma} > 1.0\ GeV$ associated with a strip camber cluster and no tracks pointing to the tower. The cluster position and the interaction vertex define the photon direction, this together with the calorimeter energy measurement determines the photon momentum. The mass difference, ΔM, between the dimuon-photon mass and the dimuon mass is shown in Figure 3 ,a peak of 1230 ± 71 events is observed at the mass of about 400 MeV/c^2 corresponding to the χ_c states. The width of the signal is about 60 MeV/c^2, too large to distinguish the χ_c^1 and χ_c^2 separated by 45.7 MeV/c^2. The statistics allow to observe a significative signal dividing the sample in four J/ψ p_T bins.

We obtain the shape of the background with a Monte Carlo method that uses the real J/ψ events as input. Each charged track in the event is assumed to be a π^0 , η or K_s in ratios predicted by the measured K/π and η/π^0 ratios and isospin symmetry. The particles are decayed and the resulting photons simulated through the detector. Applying the χ_c reconstruction to this event gives a ΔM distribution that is our model for the shape of the background. The number of signal events is extracted fitting the data to the sum of a gaussian and this background shape. To test this model we compared the ΔM distribution obtained in this way with the one directly obtained from the data, both for dimuon pairs in the sidebands of the J/ψ peak where there is no χ_c signal. The agreement is very good for every J/ψ p_T bin.

The photon reconstruction efficiency is obtained using conversion electrons found in the data an correcting for the known differences in detector response between photons and electrons. After correcting for the the photon acceptance and reconstruction efficiency we obtain a fraction of J/ψ from χ_c of $28 \pm 1.6 \pm 6.8\%$. This fraction includes a contribution from $B \rightarrow J/\psi X$ and $B \rightarrow \chi_c X$ that must be removed. We do this using the cross section of J/ψ from b's measured by CDF and the branching ratios of B mesons to charmonium states measured by CLEO. This correction is small, the fraction of J/ψ from χ_c without the contribution from b's is $32 \pm 2.0 \pm 8.5\%$ and is shown as function of J/ψ p_T in Figure 4. Figure 5 shows the cross section for J/ψ from χ_c and for direct J/ψ , both with the b contribution removed. The J/ψ from χ_c cross section is in agreement with the theoretical calculation while the direct J/ψ data is again a factor ~ 50 over the prediction.

We conclude that the color singlet perturbative QCD model of charmonium production fails to describe direct production, both for the $\psi(2S)$ and the J/ψ by about the same large amount. Contrary to its prediction direct production is the dominant source of prompt $\psi(2S)$ and J/ψ . This data does not exclude the possibility of a contribution from $c\bar{c}$ states above the open charm threshold, but makes this an unlikely explanation for the large excess of direct $\psi(2S)$ and J/ψ . It has been shown that the inclusion of the color octet mechanism establishes agreement with the data, although introducing parameters not calculable within the model and derived from the fit to the data [10].

As noted earlier this analysis has insufficient resolution to distinguish the two χ_c states. A complementary analysis can be done requiring that the photon has converted into an e^+e^- pair. With this method the photon reconstruction uses only tracking information greatly improving the χ_c mass resolution. The efficiency of this reconstruction is low, therefore this analysis utilizes a larger data sample corresponding to $75pb^{-1}$. Events are selected requiring the photon to have $p_T > 1.0GeV/c$ and a conversion vertex separated from the primary interaction vertex by more than 1.0cm in the transverse plane. To select prompt χ_c candidates we use only J/ψ reconstructed in the SVX and require $c\tau_{pseudo} < 100\mu m$. The resulting $J/\psi\gamma$ mass distribution is shown in Figure 6. The χ_c^1 and χ_c^2 peaks, with 46 ± 7 and 23 ± 6 events respectively, are nicely separated. These rates, with a small acceptance correction and the known decay branching ratios, are used to obtain the relative production cross section of:

$$\frac{\sigma(\chi_c^2)}{\sigma(\chi_c^1) + \sigma(\chi_c^2)} = 0.47 \pm 0.08(stat) \pm 0.02(sys)$$

2.3 Υ

In the $b\bar{b}$ system CDF has measured the differential cross section for the Υ 's. In $17pb^{-1}$ of data we have reconstructed $\sim$ 1200 $\Upsilon(1S)$, $\sim$ 300 $\Upsilon(2S)$ and $\sim$ 200 $\Upsilon(3S)$. The production cross sections measured in the rapidity range $\mid y \mid < 0.4$ are:

$$\sigma(\Upsilon(1S)) = (23.48 \pm 0.99 \pm 2.80) \text{ nb}, \; p_t > 0.5 \; GeV/c$$
$$\sigma(\Upsilon(2S)) = (10.07 \pm 1.01 \pm 1.99) \text{ nb}, \; p_t > 1.0 \; GeV/c$$
$$\sigma(\Upsilon(3S)) = (4.79 \pm 0.64 \pm 0.72) \text{ nb}, \; p_t > 1.0 \; GeV/c$$

The differential cross sections are shown in Figure 7. The theoretical curve is a leading order QCD calculation that includes the contributions from all the known χ_b states and feed-down from the S states. The measured cross sections are higher than the calculations by a factor ~ 3 for the $1S$ and $2S$ and ~ 10 for the $3S$. For the Υ 's the experimental analysis, at this time, is not as complete as it is in the charmonium system because the contribution from the χ_b's has not been separated. The lower statistics have not allowed the reconstruction of the radiative decay of the χ_b yet. Therefore a conclusion on the origin of the disagreement can not be definitively drawn. For the Υ 's the shape of the differential cross section is also not reproduced by the calculation in the low p_T region, but it has been shown that including a parton k_T smearing agreement in the shape can be obtained [10]. Unfortunately also this effect cannot be quantitatively calculated and must be derived from a fit to the data.

3 Charmonium Production at Fixed Target

3.1 E789

In this experiment the primary 800 GeV/c proton beam was incident upon a thin, 3mm long, gold target. Charged particles resulting from the interaction were magnetically deflected around a beam dump suspended within the first analyzing magnet. A second magnet downstream provided the momentum measurement and confirmed the association of the track with the interaction point. Muon detectors were located behind a thick absorber wall [11]. The acceptance was limited to the small Feynman-x range: $-0.03 < x_F < 0.15$.

In the data analysis a pair of opposite sign muons was required and the two tracks were constrained to originate from the target. The resulting mass resolution for the J/ψ was 16 MeV/c^2. The differential cross sections were derived from 112649 ± 486 J/ψ and 1824 ± 114 $\psi(2S)$. These are shown in Figure 8 compared with the leading order perturbative QCD calculation. While the prediction and the data show reasonable agreement in shape if the proper k_T smearing is used, the theoretical calculations have been increased by a K factor equal to 7 for the J/ψ and 25 for the $\psi(2S)$ in order to get agreement in magnitude [12]. It is interesting to notice that the K factors needed to bring the theoretical calculation in agreement with the CDF data, $p\bar{p}$ at $\sqrt{s} = 1.8$ TeV , are the same of these, p-Nucleon at $\sqrt{s} = 39$ GeV , within a factor of two.

3.2 E705

This experiment used 300 GeV/c positive (45% $\pi^\pm$ and 55% p) and negative (98% $\pi^\pm$ and 2% $\bar{p}$) beams. The beam was aimed at a 33cm long lithium target. Two beam-line Cerenkov counters tagged the beam particle type on an event by event basis. The large acceptance spectrometer included magnetic analysis of charged tracks, an electromagnetic calorimeter for the photon identification and muon detectors. The Feynman-x acceptance was : $-0.10 < x_F < 0.45$. Reconstruction of the dimuon data yielded a sample of approximately 23000 J/ψ and 500 $\psi(2S)$ [13].

The J/ψ data sample was used to reconstruct the radiative decays of the χ_c 's. For this analysis the muon pair was combined with all photon candidates, other than those from reconstructed π^0 decays, with $E^\gamma > 2.5$ GeV. Figure 9 shows the resulting ΔM distribution for $\pi^\pm$ and proton beams. To measure the relative χ_c^1/χ_c^2 production rate a simultaneous likelihood fit to the two mass plot was performed. The χ_c^1 and χ_c^2 resolution function used was derived from the Monte Carlo simulation. Correcting for the known decay branching ratio the result is $\sigma(\chi_c^1)/\sigma(\chi_c^2) = 0.52^{+0.57}_{-0.27}$ for the $\pi^\pm$ beam and $\sigma(\chi_c^1)/\sigma(\chi_c^2) = 0.08^{+0.25}_{-0.15}$ for the proton beam [14].

The suppression of χ_c^1 production in p-Nucleon production, at the low p_T typical of fixed target experiments, is predicted by the QCD color singlet model. This is because, at leading order, only gluon-gluon fusion contributes to χ_c production and the χ_c^1 , a 1^{++} state, can not couple to two gluons. In this case the experimental result is in agreement with the theoretical prediction, on the other hand the two χ_c states in this analysis are not cleanly separated and the uncertainties are large.

This experiment has also performed a thorough study of the sources of J/ψ mesons for each beam particle type. From the number of reconstructed J/ψ and χ_c , correcting for the photon acceptance, E705 measures the fraction of J/ψ arising from χ_c decays. Another contribution to J/ψ production is $\psi(2S)$ production followed by decay into final states containing J/ψ . To obtain this fraction the measured J/ψ and $\psi(2S)$ cross sections together with the known decay branching ratios are used. The results are summarized in Table 1 together with the $\psi(2S)$ / J/ψ cross section ratio. The direct J/ψ is the fraction not from χ_c or $\psi(2S)$ [15].

beam	$\sigma(\psi')/\sigma(\psi)$	F_χ^ψ	direct ψ	from ψ'
π^+	0.12 ± 0.04	0.40 ± 0.04	0.54 ± 0.05	0.064 ± 0.022
π^-	0.14 ± 0.03	0.37 ± 0.03	0.56 ± 0.03	0.075 ± 0.017
p	0.14 ± 0.03	0.30 ± 0.04	0.62 ± 0.04	0.075 ± 0.017
$\bar{p}$	0.25 ± 0.22			

Table 1.

The fraction of J/ψ from χ_c is comparable with what found by CDF at a much higher $\sqrt{s}$, $F_\chi^\psi(CDF) = 32 \pm 2.0 \pm 8.5\%$. A large direct J/ψ component is necessary to describe the data, as for CDF and the ratio of $\psi(2S)$ to J/ψ production is also similar to the CDF value of 0.19 ± 0.05.

3.3 E672/706

This experiment was performed with a 515 GeV/c π^- beam incident on berillium and copper targets. The spectrometer [16] had the capability of studying high mass dimuon pairs in the Feynman-x range of: $0.10 < x_F < 0.80$. A sample of 9600 ± 105 J/ψ and 270 ± 35 $\psi(2S)$ was obtained.

The production of J/ψ from $\psi(2S)$ and χ_c was studied. From a sample of 220 ± 43 reconstructed $\psi(2S) \rightarrow J/\psi\pi^+\pi^-$ decays, correcting for the $\psi(2S)$ reconstruction efficiency and the known ratio of branching ratio $Br(\psi(2S) \rightarrow J/\psi X)$ / $Br(\psi(2S) \rightarrow J/\psi\pi^+\pi^-)$, the fraction of J/ψ from $\psi(2S)$ was obtained. To study the production from χ_c and reach the mass resolution necessary to separate the χ_c^1 and χ_c^2 states only photons that had converted into an e^+e^- pair were used. Figure 10 shows the $\mu^+\mu^-\gamma$ mass distribution. Two nicely separated peaks corresponding to the χ_c^1 and χ_c^2 with 47 ± 12 and 37 ± 11 events respectively are observed. From this the relative production rate of $\sigma(\chi_c^1)/\sigma(\chi_c^2) = 0.63 \pm 0.25$ was derived together with the fraction of J/ψ from χ_c^1 and χ_c^2 . Unfortunately this experiment has not collected data with a proton beam that can be used to measure the χ_c^1 / χ_c^2 ratio with this precision. The fractions are summarized in Table 2.

beam	$F_{\chi^1}^\psi$	$F_{\chi^2}^\psi$	direct ψ	from ψ'
π^-	0.26 ± 0.07	0.20 ± 0.06	0.45 ± 0.09	0.08 ± 0.02

Table 2.

The rate of $\sigma(\chi_c^1)/\sigma(\chi_c^2) = 0.63 \pm 0.25$ corresponds to $\sigma(\chi_c^2)/(\sigma(\chi_c^1)+\sigma(\chi_c^2)) = 0.61 \pm 0.10$, higher, but not too different from the CDF measurement.

This experiment has compared these results with a theoretical calculation [17] and good agreement was found. The model used in this calculation includes effect not included in the standard Perturbative QCD one.

4 Conclusions

Recent data on J/ψ ,$\psi(2S)$,χ_c and Υ production has unraveled surprises. The theoretical model based on perturbative QCD, previously believed to give a reasonable description of quarkonia production, dramatically fails to reproduce the data. By disentangling all production sources (from b's and direct, for the $\psi(2S)$; from b's from χ_c 's and direct, for the J/ψ) CDF found that direct production is the main production mechanism of prompt J/ψ and $\psi(2S)$ in disagreement with the expectations by a factor of 50. Fixed target data on charmonium production show a remarkably similar patter and have been available for a long time before the discovery of the "CDF $\psi(2S)$ anomaly", but, for reasons hard to understand within a Galileian approach, these data did not stimulate much theoretical interest.

From the experimental point of view more can be learned at collider experiments by studying production in the $b\bar{b}$ system separating direct Υ from feed-down from χ_b. Fixed target experiments have the possibility of testing a crucial prediction of the theory, namely the suppression of the χ_c^1 in proton-Nucleon production. At the moment this prediction seem to be confirmed by the experiments but the data are not yet clean enough for a firm conclusion.

References

[1] R. Baier and R. Ruckl, *Z.Phys.* C19 (1983) 251
E.W.N. Glover, A.D. Martin, W.J. Stirling, *Z.Phys.* C38 (1988) 473.

[2] E.Braaten and T.C. Yuan, *Phys.Rev.Lett.* 71 (1993) 1673.

[3] E. Braaten, *et al., Phys.Lett.* B333 (1994) 548.
M.Cacciari, M.Greco *Phys. Rev. Lett.* 73 (1994) 1586.

[4] UA1 Coll.,C. Albajar *et al., Phys.Lett.* B256 (1991) 112.
CDF Coll.,F. Abe *et al., Phys.Rev.Lett.* 69 (1992) 3704.
CDF Coll.,F. Abe *et al., Phys.Rev.Lett.* 71 (1993) 2537.

[5] C. Korkoumelis *et al., Phys.Lett.* B81 (1979) 405.
Y. Lemoigne *et al., Phys.Lett.* B113 (1982) 509.
S.R. Hahn *et al., Phys. Rev.* D30 (1984) 671.
D.A. Bauer *et al., Phys.Rev.Lett.* 54 (1985) 753.

[6] F. Abe *et al., Nucl. Instrum. Methods* A271 (1988) 387

[7] D. Amedei *et al., Nucl. Instrum. Methods* A350 (1994) 73

[8] F.E.Close , *Phys.Lett.* B342 (1995) 369.
D.P.Roy and Sridhar , *Phys.Lett.* B345 (1995) 537.
P.Cho and M.Wise , *Phys.Lett.* B346 (1995) 129.

[9] E.Braaten and S.Fleming *Phys.Rev.Lett.* 74 (1995) 3327.

[10] M.Mangano, these proceedings.
M.Cacciari *et al.* CERN-TH/95-129.

[11] D.E.Jaffe *et al., Phys. Rev.* D40 (1989) 2777.

[12] M.H.Schub *et al.* FERMILAB-PUB-95/058-E, Submitted to Phys. Rev. D

[13] L.Antoniazzi *et al., Phys. Rev.* D46 (1992) 4828.

[14] L.Antoniazzi *et al., Phys. Rev.* D49 (1994) 543.

[15] L.Antoniazzi *et al., Phys. Rev. Lett.* 70 (1993) 383.

[16] G.Alverson *et al., Phys. Rev.* D480 (1993) 5.
R.Jesik *et al., Phys. Rev. Lett.* 74 (1995) 495.

[17] G.A.Schuler CERN-TH.7170/94 submitted to *Physics Reports*.

List of Figures

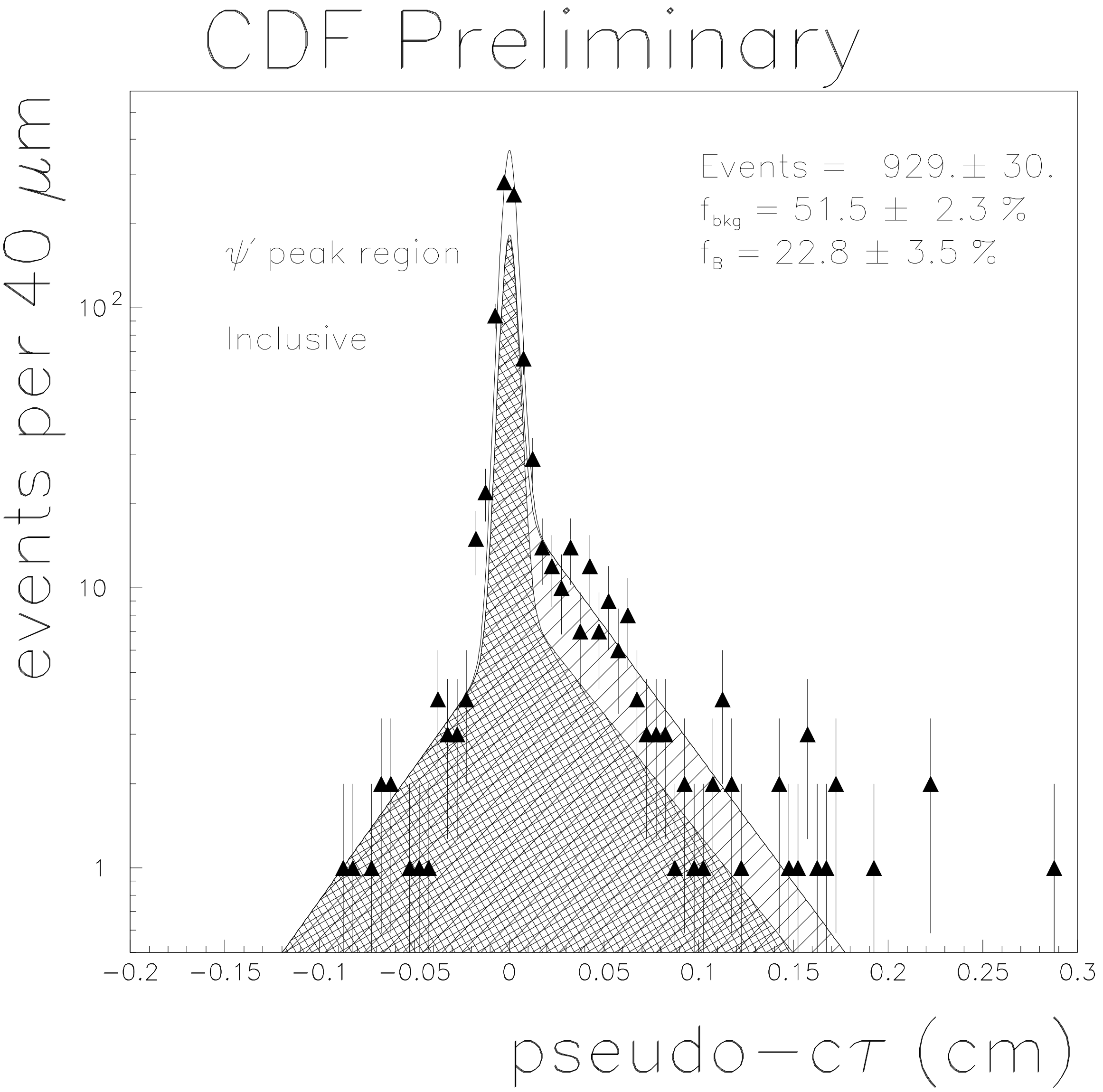

Figure 1: $c\tau_{pseudo}$ distribution for the $\psi(2S)$ decomposed into prompt (unshaded), from b decays (hatched), and background (dark shading).

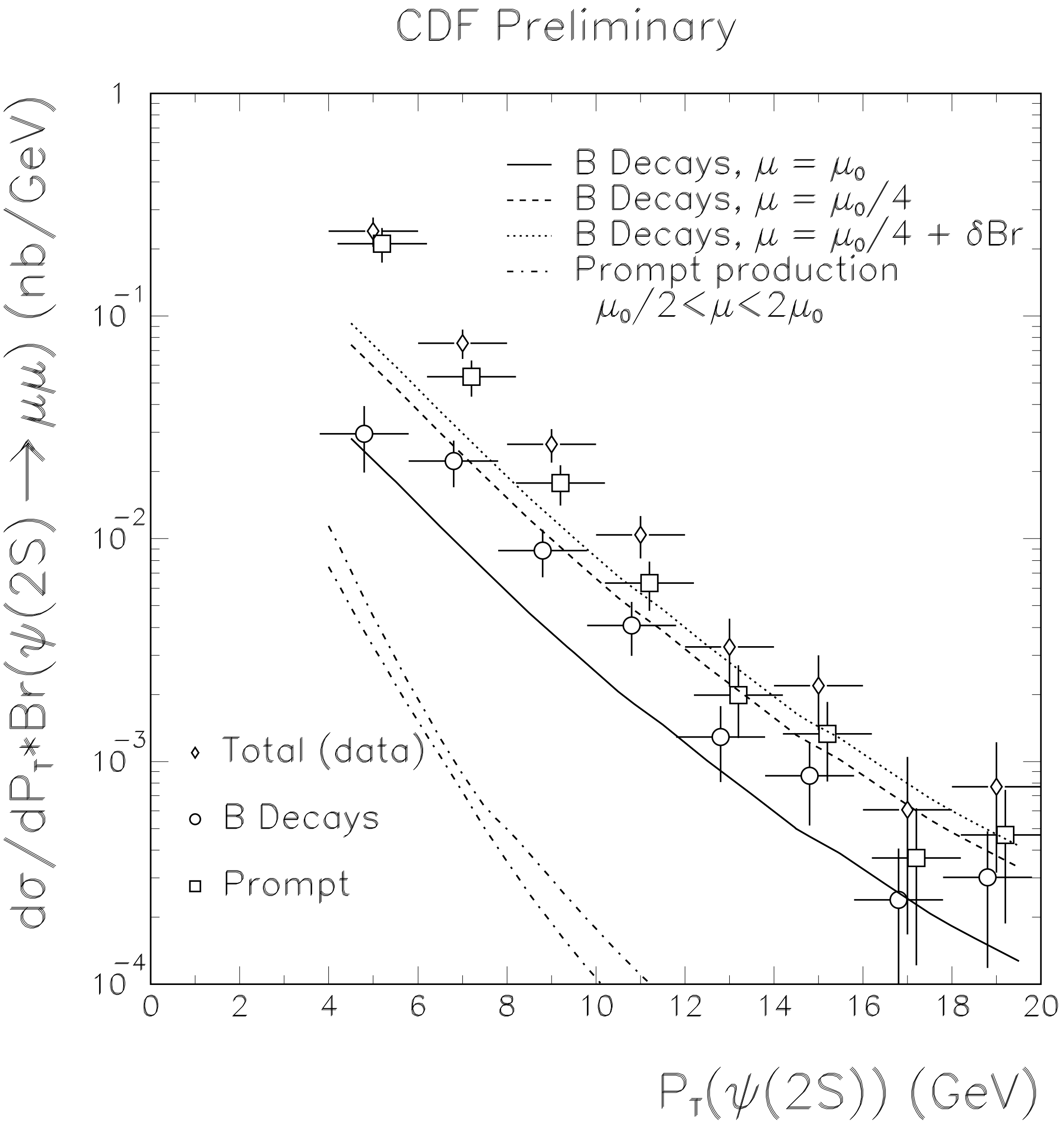

Figure 2: $\psi(2S)$ differential cross section. The curves are NLO QCD calculations.

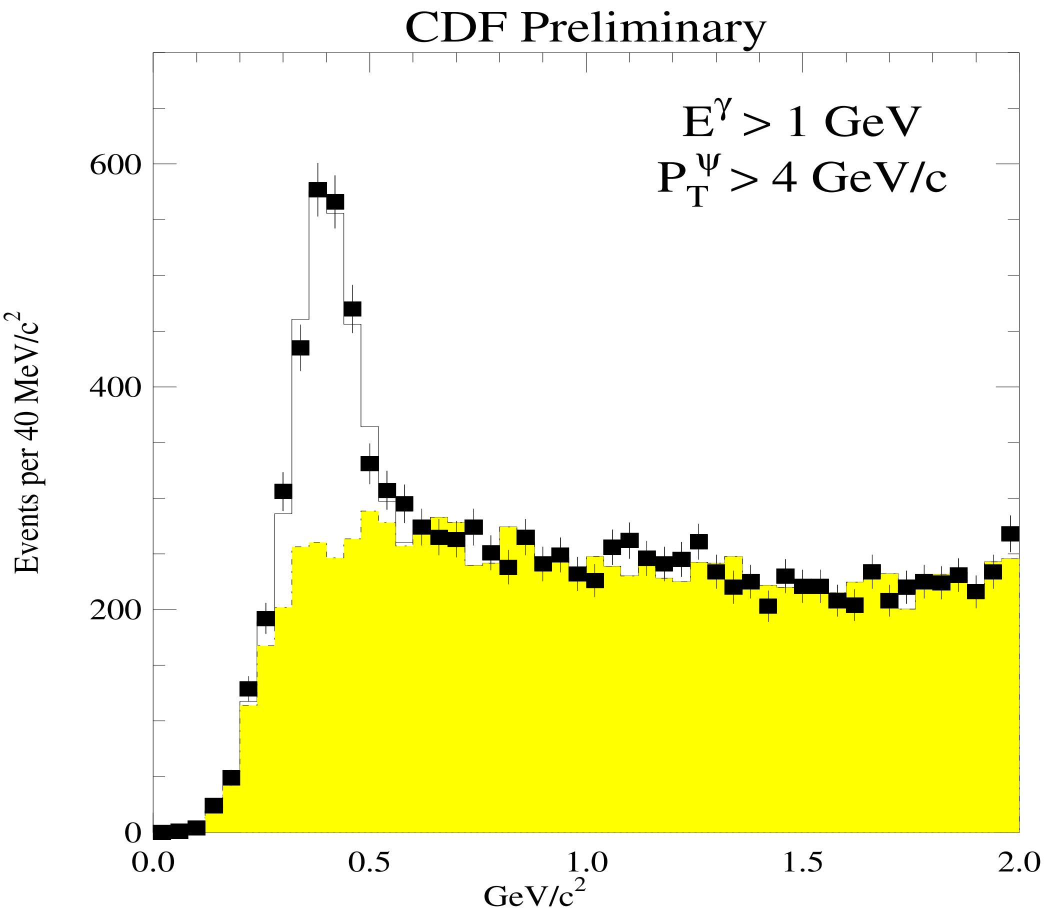

Figure 3: Mass difference $M(\mu^+\mu^-\gamma) - M(\mu^+\mu^-)$ for the ψ signal region in 40 MeV/c^2 bins. The points show the data histogram, the shaded histogram is the background shape predicted by our background Monte Carlo. The solid line is the fit to the data of a gaussian signal plus the background histogram.

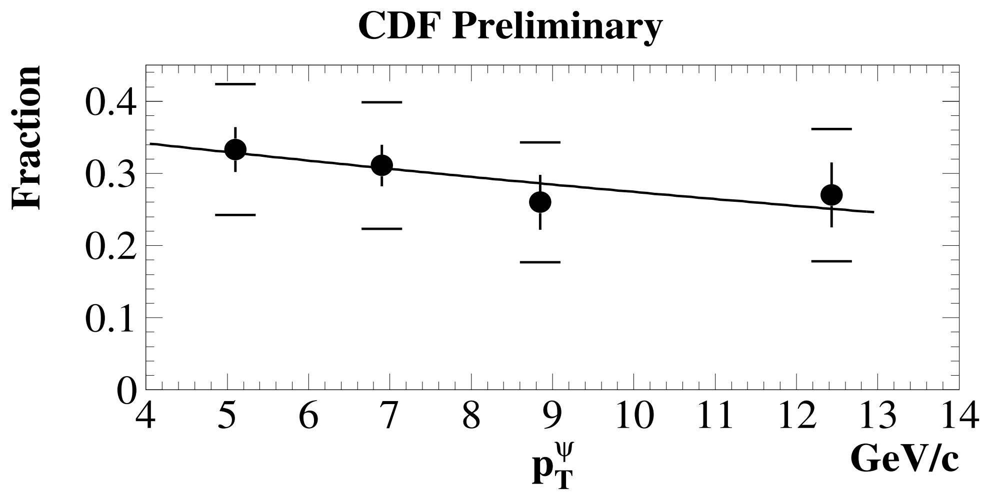

Fraction of J/ψ from χ_c vs $p_T^{J/\psi}$ with the contribution from b's removed.

$P_T^\psi > 4.0\,GeV/c$	$0.323 \pm 0.020 \pm 0.085$
$4.0 < P_T^\psi < 6.0\,GeV/c$	$0.333 \pm 0.031 \pm 0.085$
$6.0 < P_T^\psi < 8.0\,GeV/c$	$0.311 \pm 0.029 \pm 0.083$
$8.0 < P_T^\psi < 10.0\,GeV/c$	$0.260 \pm 0.038 \pm 0.074$
$P_T^\psi > 10.0\,GeV/c$	$0.270 \pm 0.045 \pm 0.080$

Figure 4: Fraction of J/ψ from χ_c as function of the J/ψ p_T with the contribution from b's removed.

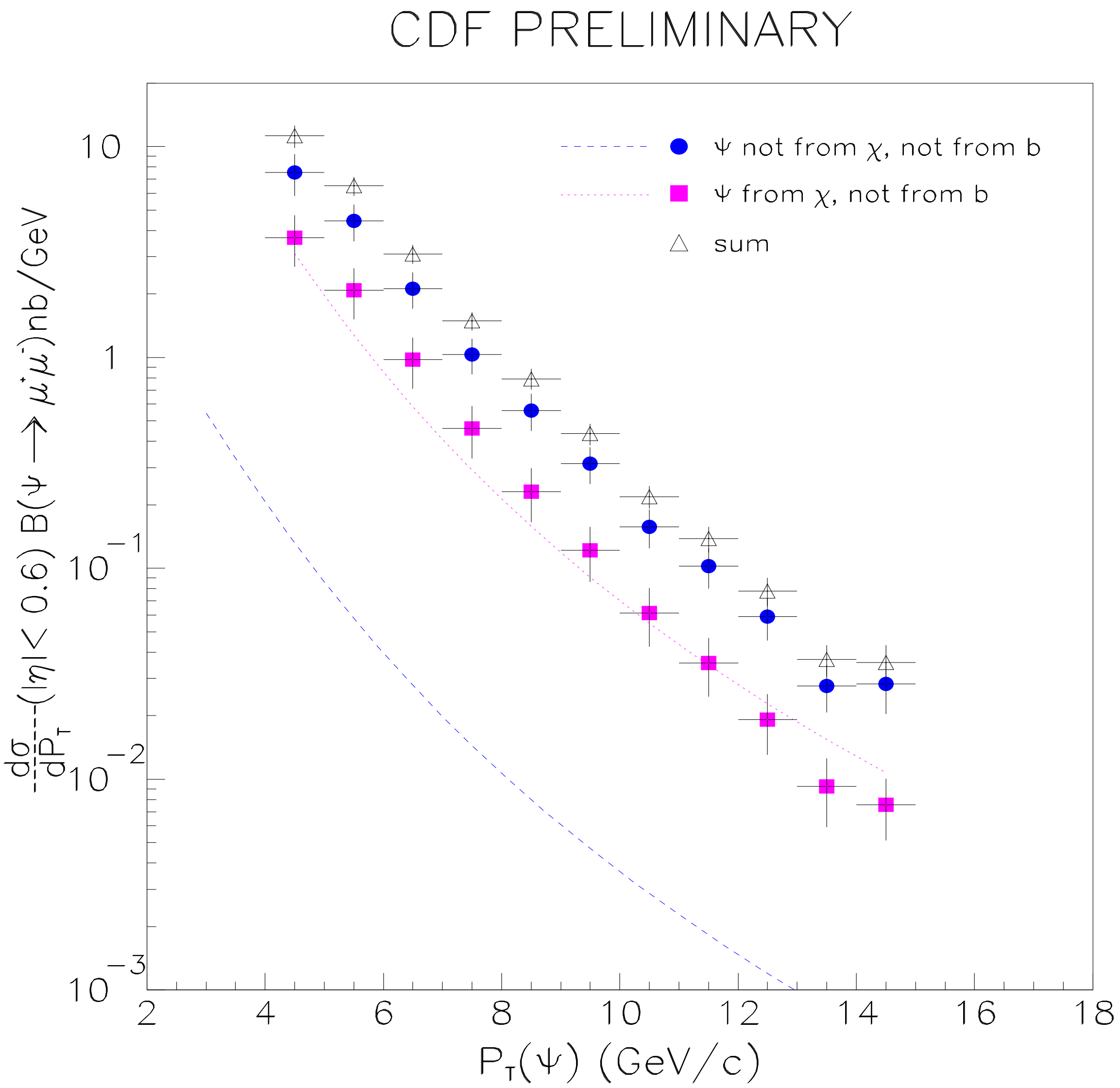

Figure 5: J/ψ differential cross sections as a function of J/ψ p_T with the contribution from b's removed; the circles show the direct component, the squares correspond to J/ψ from χ_c and the triangle is the sum. The curves are the NLO QCD calculations.

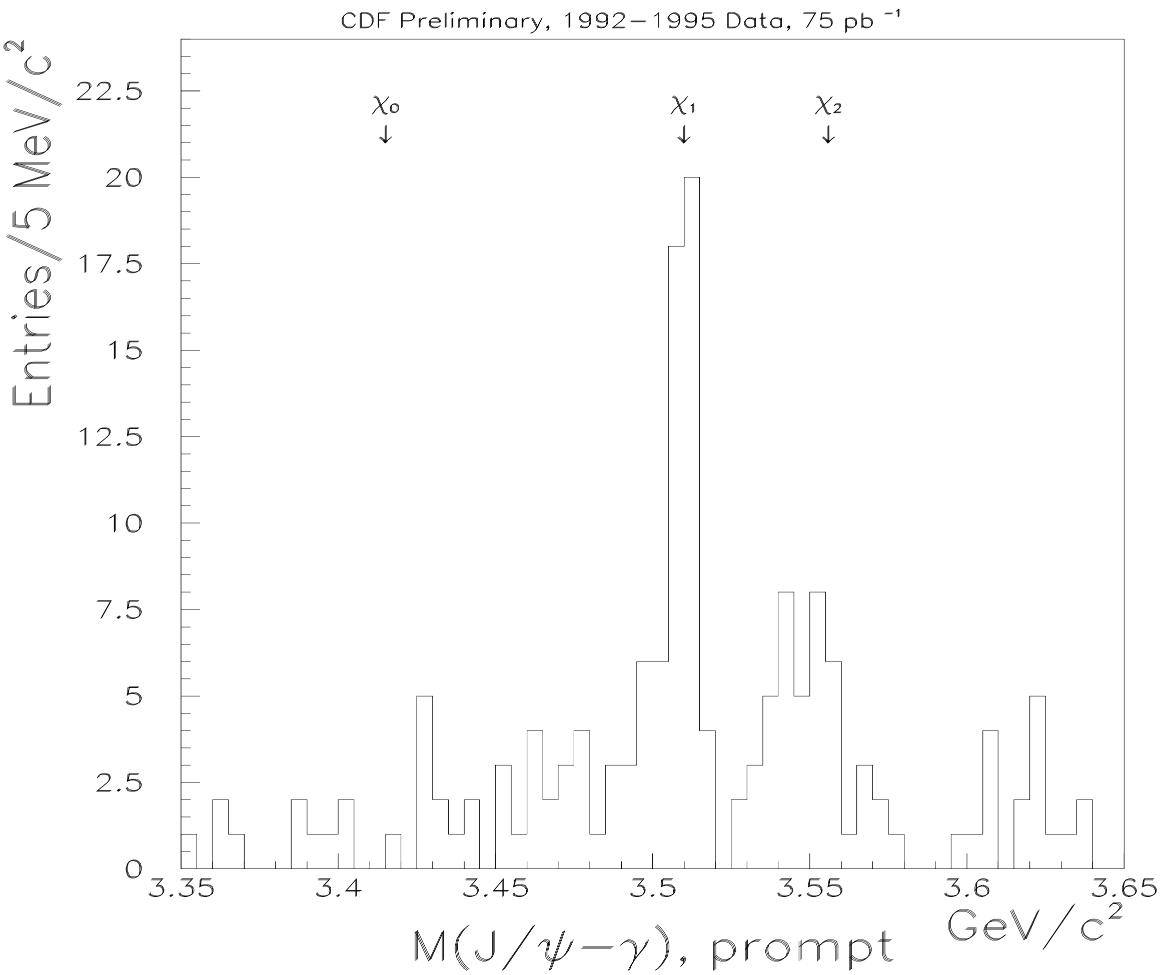

Figure 6: The $J/\psi\gamma$ mass distribution, based on tracking measurement via photon conversion, for prompt J/ψ .

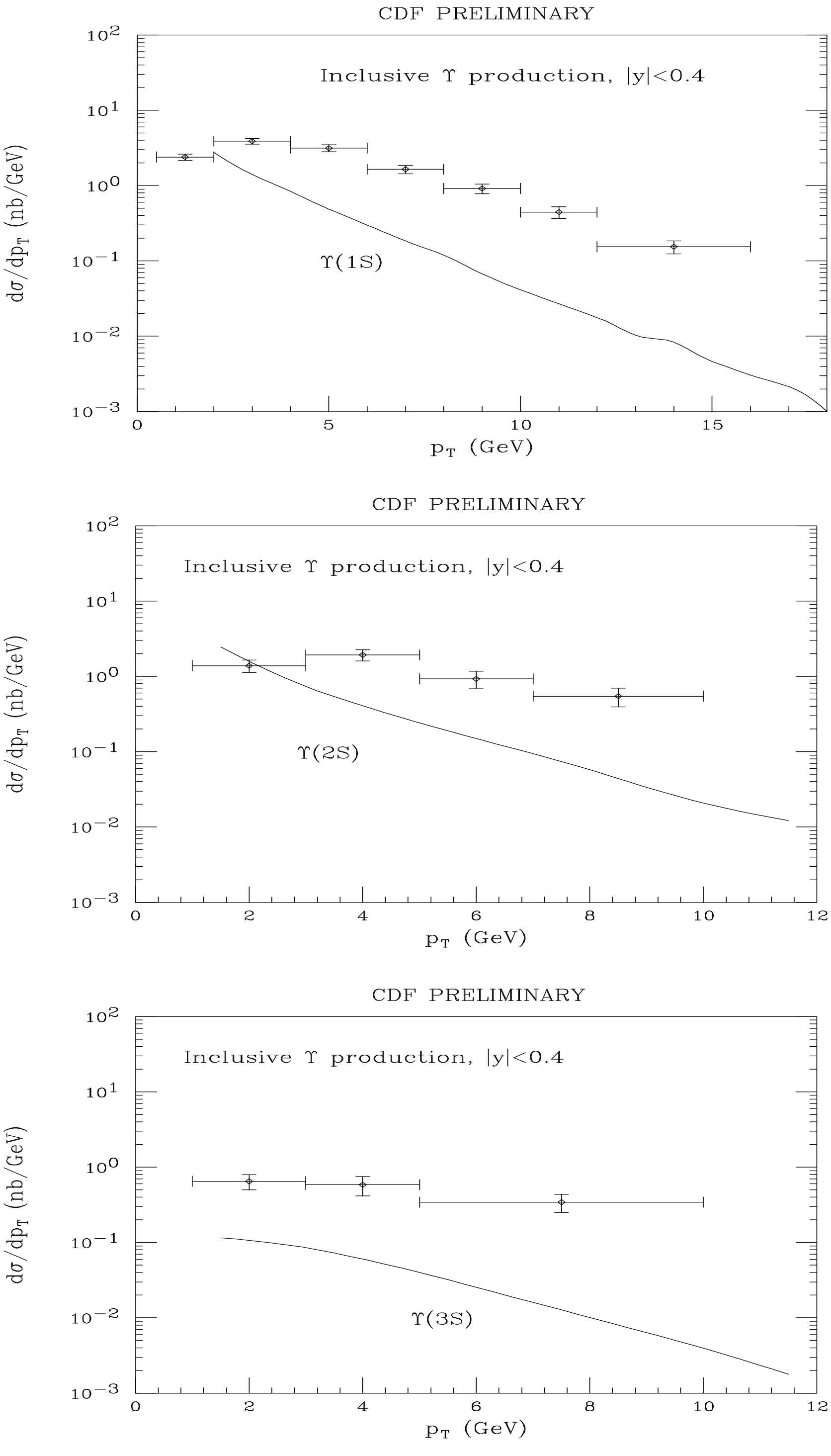

Figure 7: Υ differential cross sections as a function of p_T The curves are the LO QCD calculations.

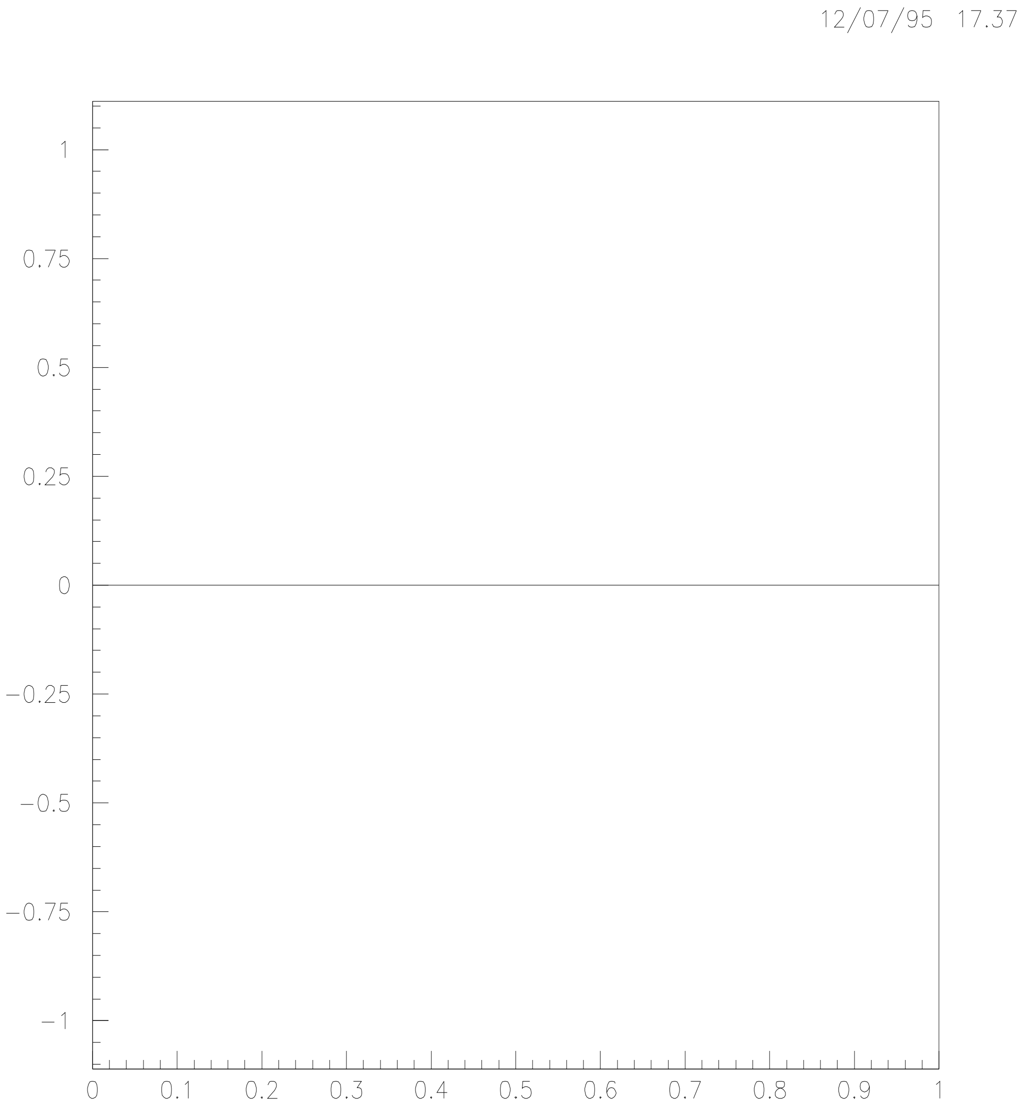

Figure 8: Differential cross section for J/ψ and $\psi(2S)$ measured by the E789 experiment. The leading-order predictions with K factors of 7 and 25 for the J/ψ and $\psi(2S)$ respectively are also shown.

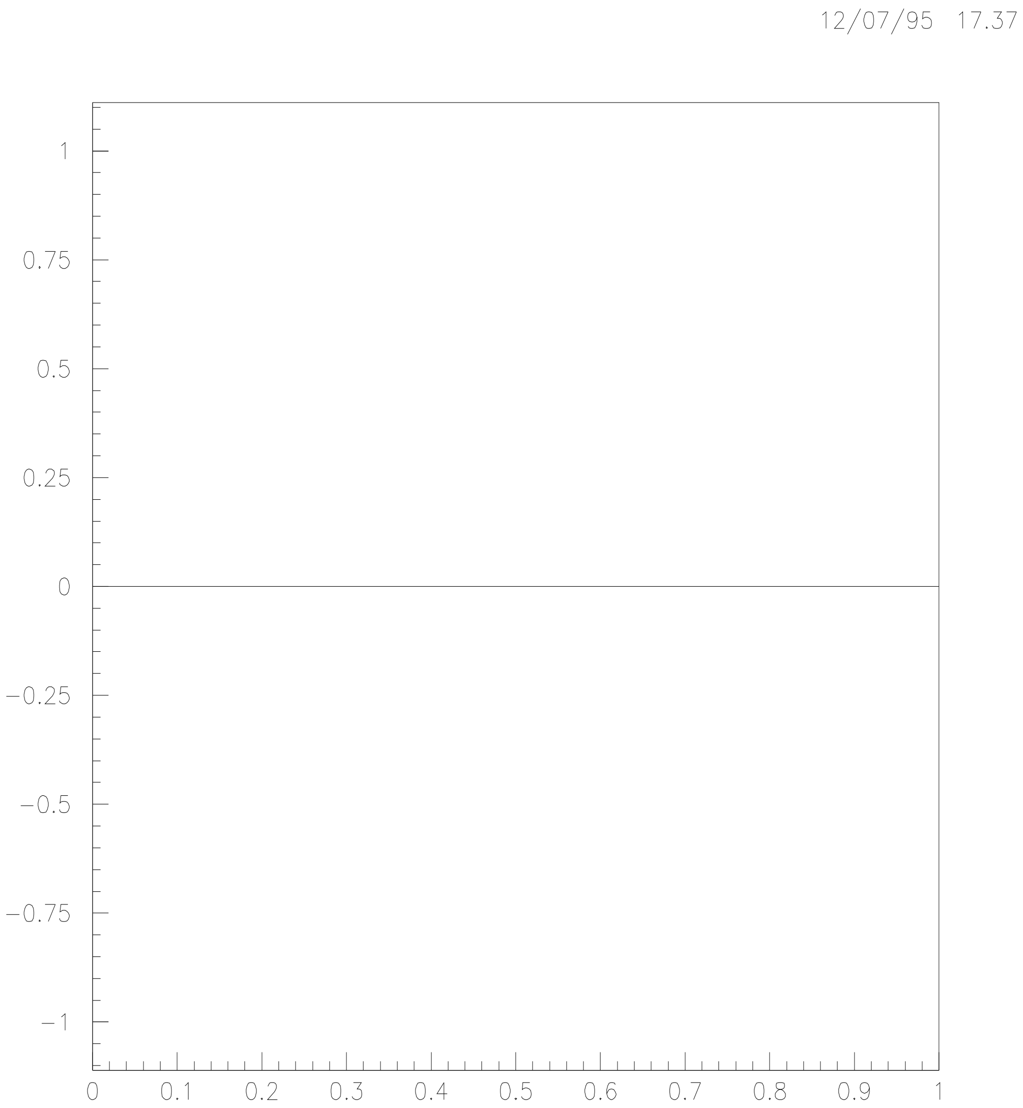

Figure 9: The $M(\mu^+\mu^-\gamma) - M(\mu^+\mu^-)$ distribution for $\pi^\pm$ and p induced reactions obtained by the E705 experiment. The smooth curves are from the likelihood fit, and the insets show the background subtracted χ_c signal.

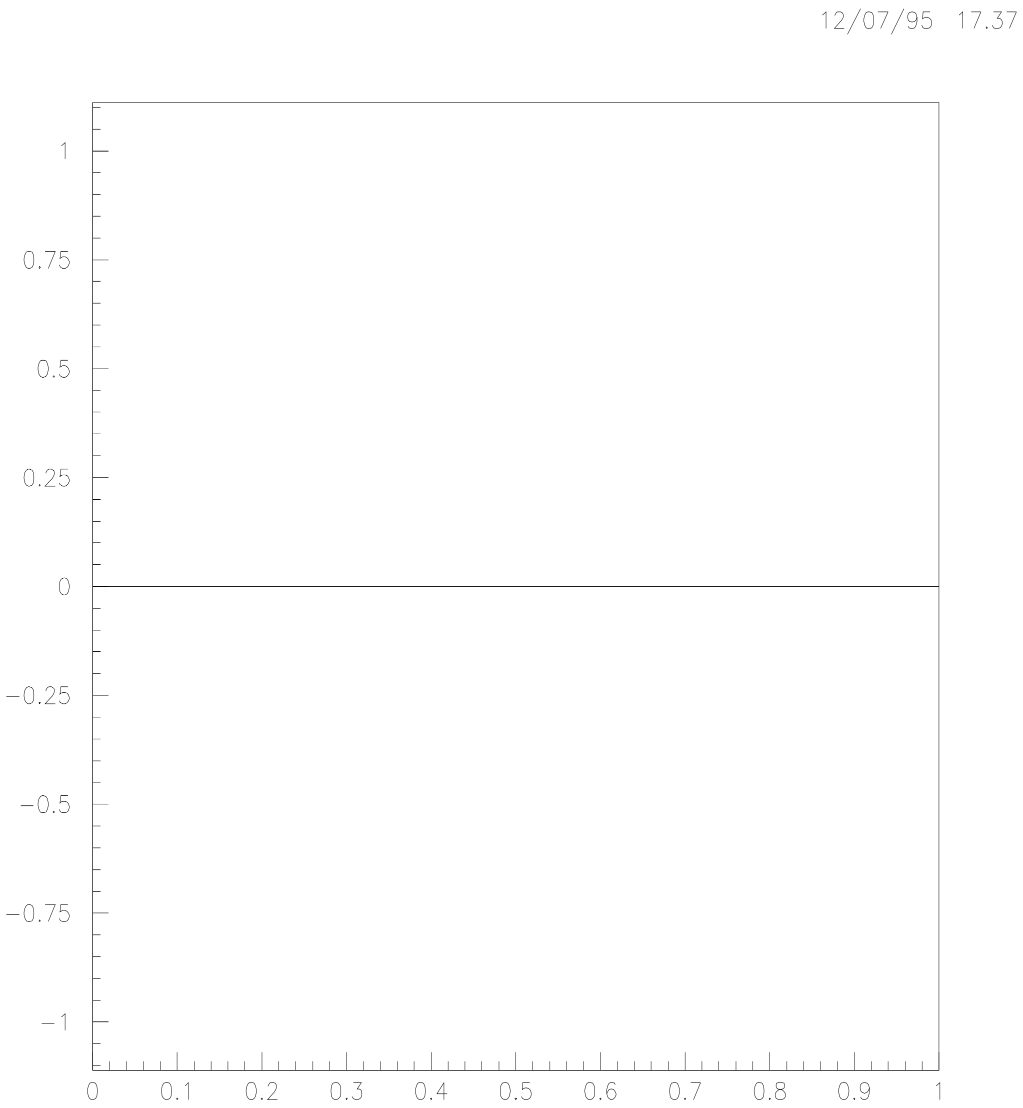

Figure 10: The $J/\psi\gamma$ mass distribution, based on tracking measurement via photon conversion, obtained by the E672/706 experiment. The solid line shows the fit to the data. The lower histogram shows the background subtracted signal.